BIBECHANA
Vol. 23, No. 1, January 2026, 86-92

ISSN 2091-0762 (Print), 2382-5340 (Online)
Journal homepage: http://nepjol.info/index.php/BIBECHANA
Publisher: Dept. of Phys., Mahendra Morang A. M. Campus (Tribhuvan University)Biratnagar

Generation and characterization of plasma jet and its effect on seeds

Bablu Kant Thakur[1], Arun Kumar Shah[2], Ram Lal Sah[2]
Reeta Silpakar[3], Rajendra Shrestha[2,4], Lekha Nath Mishra[2,*]
[1]*Department of Physics, Trichandra Multiple Campus, Tribhuvan University, Nepal*
[2]*Department of Physics, Patan multiple campus, Tribhuvan University, Nepal*
[3] *Department of information Technology, Nepal Banepa Polytechnic Institute, Banepa, Nepal*
[4]*Department of Physics, Nepal Banepa Polytechnic Institute, Banepa, Nepal*

[*]Corresponding author. Email: lmishra@gmail.com

Abstract

These days, atmospheric pressure plasma jet technology is regarded as one of the most practical instruments in a number of domains, such as agriculture, plasma medicine, and surface modification. A quartz glass tube with an internal diameter of 3 mm and an exterior diameter of 5 mm is used to create the plasma jet. The electrodes are 8 cm apart and have a width of 1.0 cm. They are composed of aluminum foil which wraps the glass tubes. As a working gas, argon is utilized. The power supply has a frequency of 27 kHz and a voltage of 20 kV. Electron density and electron temperature have been established in order to describe plasma. The stark broadening method and power balance are used to determine the electron density. The line intensity ratio method is used to determine the electron temperature. It is revealed that applied voltage and gas flow rate affect both electron density and temperature.

Keywords
Plasma jet, surface modification, electron density, stark broadening, power balance

Article information
Manuscript received: September 2, 2025; Revised: November 8, 2025; Accepted: November 23, 2025
DOI https://doi.org/10.3126/bibechana.v23i1.87181

1 Introduction

The discharges between two electrode plates in rare gases at low pressure are the most widely used artificial plasma production method. Because of the research done on plasma discharges throughout the years, scientists today consider this medium to have unique and very advantageous properties. Ions, electrons, excited atoms, photons, and other particles created inside plasma gather energy and become reactive. A cloud containing an equal number of negatively, positively, and neutrally charged particles makes up the quasi-neutral condition known as plasma. Because plasma behaves collectively, the motion of charged particles within it affects the motion of other particles; as a result, the charged particle will not exhibit single-particle motion. The collective behavior is due to the coulomb forces cre-

ated by the interaction of negative charges. Due to this property, plasma will show collective electromagnetic objects. The collective behavior property is an important factor which distinguishes plasma from solid, liquid and gas [1,2]

A new area of agriculture called "seed treatment with plasma technology" holds the potential for raising crop productivity, germination rates and seed quality [3]. The non-equilibrium atmospheric pressure plasma produced using different configurations has collected keen interest in agriculture due to its potential to enhance seedling growth and germination rate in various crops [4]. The first known case of plasma application on plant seeds was in a US patent wherein soybean seeds were treated with CAPP made from air, oxygen, and nitrogen gases, resulting in improved germination and growth [5]. Several studies have demonstrated that applying atmospheric pressure plasma to various seeds can improve germination and seedling growth [6].

For plasma production, locally available material like quartz glass tube, Aluminum foil etc. are used.

We have created a cost-effective gadget that can produce a low-temperature, non-equilibrium atmospheric pressure plasma jet. The development of the economically viable plasma jet system has several uses in material processing and medicinal research [7, 8]. The working gas is argon, and the plasma jet is produced in a quartz glass tube [9,10] We can touch such a plasma jet with our bare hands because it poses no threat to human health [11]. Techniques for plasma characterization can be used to ascertain the condition of the plasma [12, 13] Plasma is described by its electron density [14] This technique creates a plasma jet in a quartz glass tube of different sizes. The capillary tube is wrapped in aluminum foil to create the electrodes, which are 1.0 cm diameter. The separations between the electrodes are 4cm and 8cm [15–17]

In this work, such generated plasma is treated on Swiss chard seeds for different durations and its impact on such seeds for the germination and seedling growth. Not only this but also, evolution of germination is noted for the variation of gas flow rate.

2 Materials and Methods

The Swiss chard seeds were purchased locally at the market in Kathmandu. After being exposed to plasma, the Swiss Chard was maintained in a petri dish. After that, both treated and untreated seeds were planted in a seed tray with soil. Each tray carries fifty cells.

2.1 Plasma generation and its characteristics

The experimental set up to produce plasma jet is shown in Fig.1 which consists of electrode system made of aluminum foil of 1.0 cm wide, wrapped around a quartz glass tube. The upper electrode is connected to high voltage power supply while the lower electrode is grounded. The distance between two electrode is 8 cm. The flow rate of argon is maintained at 2 and 3 litre/min and voltage is maintained at 6-9 kV. Frequency is maintained at 27 kHz. The current and voltage probe are used for electrical characterization. The voltage across discharge is measured using a 1000 × voltage probe PINTEK HVP-40 and an oscilloscope (Tektronix TBS 1052B). A 100 Ω resistor is connected in series with the ground (Tektronix TPP0051, 10 × voltage probe) electrode to measure the discharge current. Optical emission of discharge is observed by HR1- high-resolution spectrometer (ASEQ Instrument) in which the optical fiber cable is placed 10.0 mm below the lowest point of the electrode.

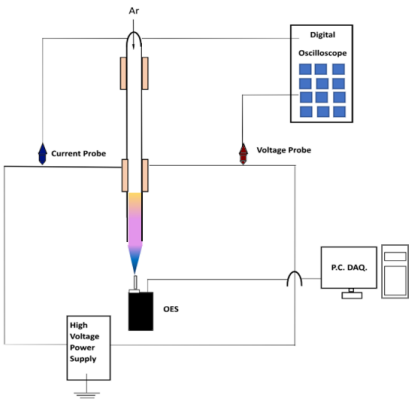

(a) Schematic Diagram of Plasma jet

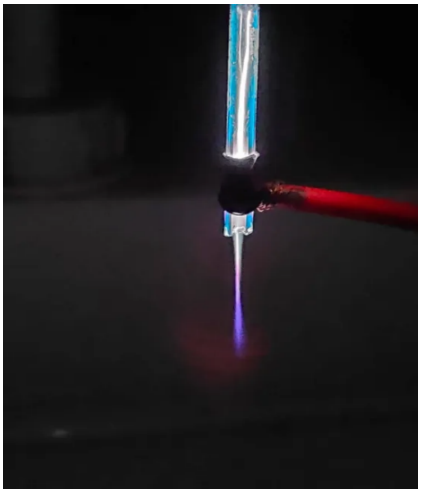

(b) Real Picture of Plasma Jet

Figure 1

3 Results and Discussion

3.1 Electrical Characterization of APPJ

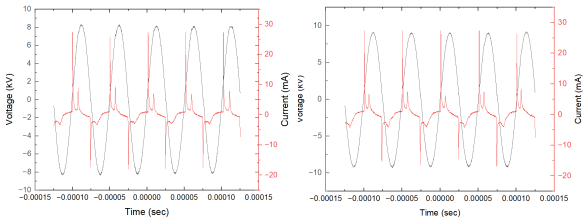

(a) (b)

Figure 2: Current-Voltage Graph

Figure 2 (a) and Fig. (b) show the discharge voltage with respect to time and 2(b) shows the discharge current with respect to time of APPJ, with electrode gap of 8 cm, applied voltage 8 kV and an operating frequency of 27kHz at atmospheric pressure condition. The electron density is determined by using power balance method expressed in eqn.(1) [18]

The glow mode discharge is homogeneously spread over the whole electrode area, so the plasma density can be estimated from a power balance method (described by Lieberman and Lichtenberg, 1994, chapter 3.5; energy lost per electron-ion pair created – Page 81 and chapter 10.2 electronegative plasma equilibrium – Page 304). The energy lost by the system per electron-ion pair can be written as:

$$E_{lost} = V_p + E_e + E_e \tag{1}$$

where V_p is the plasma potential (K.E. gained by an ion falling through the wall sheath of ∼5kTe). E_e is the K.E. of electrons lost to the wall (∼2kTe). E_{col} represents the collisional energy lost per electron-ion pair created (taking into account the ionization potential, the excitation energy lost per photon in radiation and elastic collision costs included).

E_{lost} depends on Te which is expected to be between 10 and 20 eV [19] and under these conditions E_{lost} can be reasonably approximated to 50 eV for argon [20].

The total power absorbed by a capacitively coupled plasma can be written as

$$P_{abs} = 2A_e n_e V_b E_{lost} \tag{2}$$

where $2A_e n_e V_b$ represents the total current by ion charge over the area 2A of two electrodes (A=78.5 cm^2), V_b is Bohm velocity (which equals the ion sound speed, in our condition, 2×10^5 cm/s).

$$n_e = \frac{P_{av}}{2\ AV_b E_{lost}} \tag{3}$$

Where P_{av} is the total power, A is the area of electrode, V_b is the bohm velocity and E_{lost} is the energy lost per cycle.

V_b = 2 x 10^{-3} m/s

E_{lost} = 80 x 10^{-19} J

A = 1.16 x 10^{-6} m^2

V = 5.66 kV, 6.36 kV

I = 15.84 mA, 15.70 mA

The electron density was found to be 2.41 x $10^{21}m^{-3}$ and 2.69 x $10^{21}m^{-3}$. This shows that the electron density increases with the increase in applied voltage.

3.2 Optical Characterization of APPJ:

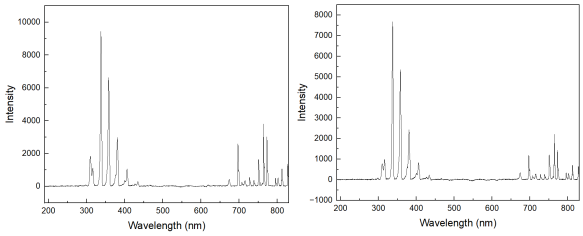

(a) (b)

Figure 3: Spectrum of discharge

The typical optical characterization of the discharge as shown in Fig. 3 was carried out by using the line intensity ratio method. In this method, two for Ar I and two for Ar II were chosen from spectral lines obtained from atmospheric glow discharge. The electron temperature is determined by using the formula [21, 22].

$$R = \frac{I_1}{I_2} = \frac{A_{ji1} g_{i1} \lambda_2}{A_{ji2} g_{i2} \lambda_1} \exp\left(-\frac{E_{i1} - E_{i2}}{K_B T_e}\right) \tag{4}$$

where, R is the ratio of the intensity of two lines, I is the intensity of spectral line, A_{ji} is the transition probability, g_i is the statistical weight of upper level, λ is the wavelength of spectral line, E_i is the energy of upper level, K_B is Boltzmann Constant, and T_e is electron temperature. The values of A_{ji}, g_i, and E_i are obtained from National Institute of Standards and Technology (NIST) Atomic Spectra Database and values of λ and I are obtained from the observation.

Table 1 represents the wavelength and their corresponding intensities obtained from observed data, The corresponding transition probability, statistical weight and energy are taken from NIST database [23, 24]

Substituting these values in eqn. (2).

Table 1: Parameters of ArI and ArII lines (taken from NIST database).

Lines	Wavelength (nm)	Transition probability (S^{-1})	Statistical Weight	Energy (eV)	Intensity (au) 2 L/min	Intensity (au) 3 L/min
Ar I	$\lambda_{pq} = 696.806$	$A_{pq} = 6.4 \times 10^6$	$g_p = 3$	$E_p = 13.327$	$I_1 = 1203.687$	$I_1 = 2596.531$
Ar I	$\lambda_{rs} = 763.7776$	$A_{rs} = 2.45 \times 10^7$	$g_r = 5$	$E_r = 13.171$	$I_2 = 2203.754$	$I_2 = 3800.631$
Ar II	$\lambda_{xy} = 316.33$	$A_{xy} = 1.8 \times 10^8$	$g_x = 4$	$E_x = 23.893$	$I_3 = 996.709$	$I_3 = 1116.082$
Ar II	$\lambda_{uv} = 380.472$	$A_{uv} = 1.5 \times 10^8$	$g_u = 6$	$E_u = 22.514$	$I_4 = 2415.21$	$I_4 = 2988.318$

The ratio of intensities is obtained as:

$$\frac{R_1}{R_2} = 0.256 \exp\left(\frac{1.223}{KT_e}\right) \tag{5}$$

$$\frac{R_1}{R_2} = 1.325 \text{ for 2 litre per minute} \tag{6}$$

$$\frac{R_1}{R_2} = 2.113 \text{ for 3 litre per minute} \tag{7}$$

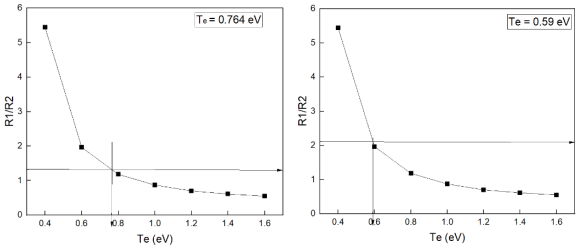

(a) (b)

Figure 4: Graph of Intensity Ratio of corresponding wavelength as the function of electron temperature. (a) 2 l/min (b) 3 l/min

The electron temperature was found to be 0.76 eV and 0.59 eV for 2 litres /min and 3 litres /min respectively. This shows that electron temperature decreases as gas flow rate increases. The faster gas flow rate increases collision due to which electron loses energy more rapidly, and hence electron temperature decreases.

3.3 Stark Broadening Method

The stark broadening method is used to determine the electron density with the help of emission spectra of the discharge. The argon line of 696.54 nm was chosen. By using eqn. (4), the electron density can be calculated by full width half maximum (FWHM)

$$\Delta\lambda_{stark} = 2\omega\left[\frac{n_e}{10^{16}}\right] + 3.5\alpha\left[\frac{n_e}{10^{16}}\right]^{1/4} - \left[1 - \frac{3}{4}N_D^{-1/3}\right]\omega\left[\frac{n_e}{10^{16}}\right] \tag{8}$$

Where $\Delta\lambda_{stark}$ is the full width half maxima FWHM, ω is the electron impact parameter, α is the ion broadening parameter, n_e is the electron density (cm^{-3}), T_e is the electron temperature. Both ω and α are tabulated for different temperature. The first part of equation (2) represents the broadening due to electron contribution, while the second part represents the ion broadening. Since the ionic contribution to the broadening is usually very small, it can be neglected and the following simplified formula for determining the electron density results [14, 25]

$$\Delta\lambda_{stark} = 2\omega\left[\frac{n_e}{10^{16}}\right] \tag{9}$$

$$\Delta\lambda_{stark} = 2 \times 10^{-11} n_e^{2/3} \tag{10}$$

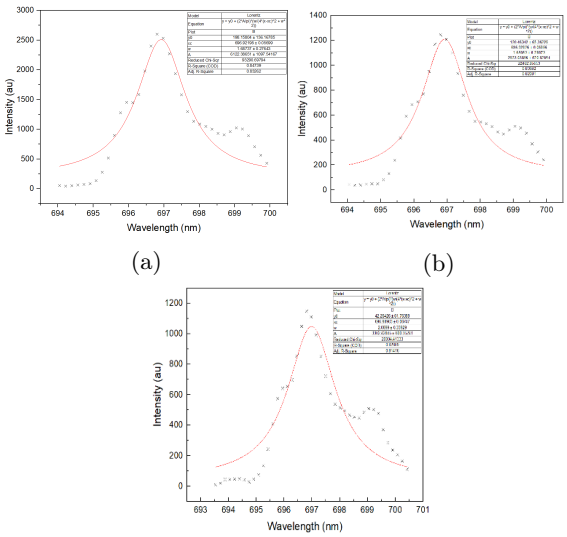

(a) (b)

(c)

Figure 5: Electron density of plasma jet (a) 2 l/min (8 kV) (b) 2 l/min (9 kV) (c) 3 l/min (8 kV)

3.4 Effect of applied voltage and gas flow rate

The stark broadening of the line of 696 nm and its Lorentzian fit is shown in Fig. 4. When gas flow rate was 2 l/min at voltage 8 kV, $\Delta\lambda_{stark} = 1.65053$ and $n_e = 2.37$ x 10^{22} m^{-3}. For gas flow rate of 2 l/min at voltage 9 kV, the value of $\Delta\lambda_{stark}$ is 2.0899 nm and electron density is 3.37 x 10^{22} m^{-3}. When the gas flow rate was 3 l/min and voltage was 8 kV, $\Delta\lambda_{stark} = 1.66796$ and $n_e = 2.405$ x 10^{22} m^{-3}. The result shows that increased gas flow rate causes

more collisions, due to which rate of ionization increases and hence electron density increases. Also, increasing applied voltage strengthens the electric field. So, electrons accelerate due to which collisions increase and hence increase electron density.

3.5 Germination of Swiss Chard

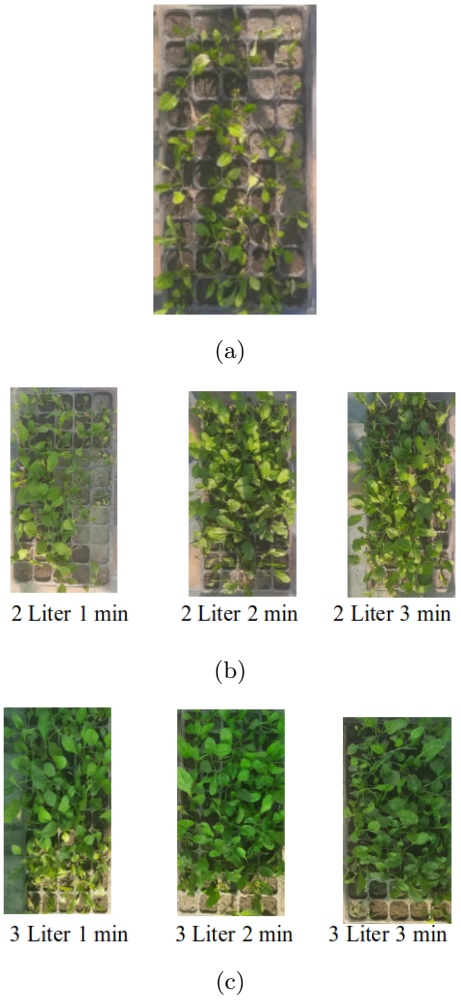

Figure 6: Germination Rate for untreated and treated seeds (a) Untreated (b) 2 L/min Treated for 1 minute, 2 minute and 3 minute (c) 3 L/min for 1 minute, 2 minute and 3 minute

The seed germination, germination rate, mean germination time and germination index of the radish seeds were calculated.

The seed germination was calculated by using:

$$\text{Germination percentage} = 100 \times \frac{\text{Number of Germinated Seeds}}{\text{Total Number of Seeds}} \quad (11)$$

The germination percentage of untreated swiss chard was found to be 62%. However, the germination percentage of the treated seeds at gas flow rate 2 L /min was found to 78%, 90%, 92% for 1 minute, 2 minutes and 3 minutes respectively. Similarly, when the gas flow rate was 3 L/min, the germination percentage was found to be 80%, 92% and 94% respectively.

The germination index (GI) was found by using:

$$GI = \frac{\text{Number of seeds germinated on 1st count}}{\text{day of the 1st count}} + \cdots + \frac{\text{number of germinated seeds on final count}}{\text{day of final count}} \quad (12)$$

It was found to be 4.81 for untreated seeds, and 6.14, 6.99, 7.38 for 2 litre 1 min, 2 litre 2 min and 2 litre 3 min treated seeds. The germination index was found to be 7.56, 7.96, 8.41 for 3 litre 1 min, 3 litre 2 min and 3 litre 3 min treated seeds respectively.

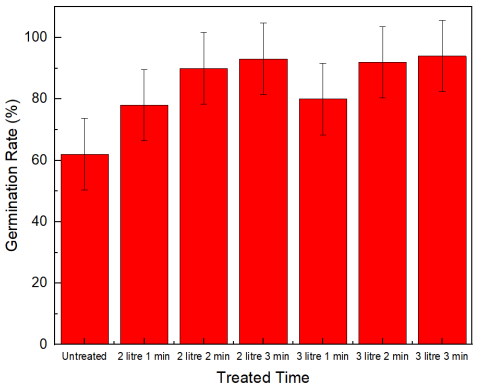

Figure 7: Germination Index for Untreated and Treated Seeds

The germination index (GI) is a frequently used metric to assess how quickly and consistently seeds germinate. In contrast to simply counting the number of seeds that germinated, it provides a more understandable indicator of seed vigor by combining germination speed and germination percentage. A higher GI indicates more rapid and consistent germination.

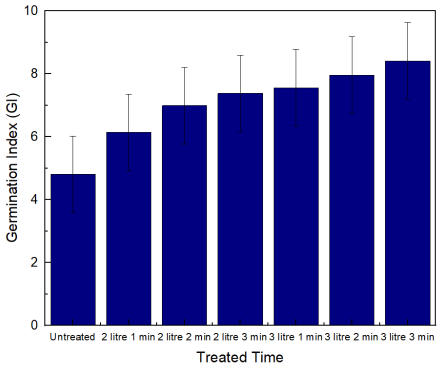

Figure 8: Germination Index for Untreated and Treated Seeds

The mean germination time (MGT) was determined by using:

$$MGT = \frac{\sum(n \times d)}{N} \tag{13}$$

where, n = number of seeds germinated on each day

d = Number of days from the beginning of the test

N = Total number of seeds germinated at the end of the test

It was found to be 8.27 for untreated seed, and 7.65, 7.41 and 7.06 at gas flow rate of 2 litres, for 1 minute, 2 minutes and 3 minutes respectively. Mean Germination Time was found to be 6.87, 6.43 and 5.85 at gas flow rate of 3 litres, for 1 minute, 2 minute and 3 minutes respectively.

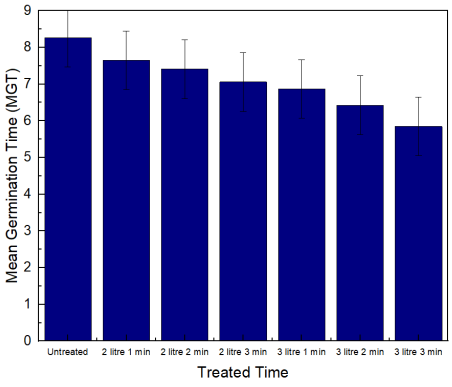

Figure 9: Mean Germination Time for Untreated and Treated Seeds

The mean germination time indicates how quickly the seeds germinate on average.

4 Conclusion

Cold Atmospheric Pressure Plasma Jet has been produced and characterized by electrical and optical methods. Electron density by electrical method was found to be 2.41 x 10^{21}m^{-3} and 2.69 x 10^{21}m^{-3} for applied voltage 8 kV and 9 kV respectively. Similarly, by optical method, when gas flow rate was 2 l/min at voltage 8 kV, electron density was found to be 2.37 x 10^{22} m^{-3}.

For gas flow rate of 2 l/min at voltage 9 kV, electron density is 3.37 x 10^{22} m^{-3}. When the gas flow rate was 3 l/min and voltage was 8 kV, electron density was 2.40 x 10^{22} m^{-3}. The electron temperature was found to be 0.76 eV and 0.59 eV when gas flow rate was 2 L and 3 L respectively. Because the stronger electric field accelerates electrons more forcefully and leads to more frequent ionizing collisions that produce more free electrons, the electron density in plasma rises with applied voltage. Additionally, a higher gas flow rate leads to more collisions, which raises ionization and, consequently, electron density. Additionally, a higher gas flow rate induces more collisions, which transfers more energy from electrons to neutral particles and lowers the temperature of the electrons. The germination parameters like germination rate, germination index of treated seed was found to be increased, and mean germination time was found to be decreased. Therefore, the germination parameter rises as a result of the drop in electron temperature and the increase in electron density. The result seems in agreement with the previous work.

References

[1] S. N. Sen. *Plasma Physics*. Anu Books, India, 2020.

[2] Francis F. Chen. *Introduction to Plasma Physics*. Springer, 1984.

[3] Rohit Thirumdas, Anjineyulu Kothakota, K. Kiran, Ravi Pandiselvam, and Vislavath Prakash. Exploitation of cold plasma technology in agriculture. *Advances in Research*, 12:1–7, 2017. doi:10.9734/AIR/2017/38044.

[4] K. Lotfy. Effects of cold atmospheric plasma jet treatment on the seed germination and enhancement growth of watermelon. *Open Journal of Applied Sciences*, 7:705–719, 2017. doi:10.4236/ojapps.2017.712050.

[5] S. A. Krapivina, A. K. Filippov, T. N. Levitskaya, and A. Bakhvalov. Gas plasma treatment of plant seeds.

[6] B. Adhikari, M. Adhikari, B. Ghimire, et al. Cold atmospheric plasma-activated water irrigation induces defense hormone and gene expression in tomato seedlings. *Scientific Reports*, 9:16080, 2019. doi:10.1038/s41598-019-52646-z.

[7] M. Konuma. *Film deposition by plasma techniques*. Springer Series on Atomic, Optical, and Plasma Physics. Springer, Berlin, 1992.

[8] J. R. Roth. *Industrial Plasma Engineering*, volume 2. IOP, Bristol and Philadelphia, 2001.

[9] A. Hamdan, J.-L. Liu, and M. S. Cha. Microwave plasma jet in water: characterization and feasibility to wastewater treatment. *Plasma Chemistry and Plasma Processing*, 38(5):1003–1020, 2018. doi:10.1007/s11090-018-9918-y.

[10] S. Fester, C. Mohr, and W. Viöl. Investigations of atmospheric pressure plasma jet by optical emission spectroscopy. *Surface and Coatings Technology*, 200(4):827–830, 2005. doi:10.1016/j.surfcoat.2005.02.217.

[11] D. L. Pavia, G. M. Lampman, and G. S. Kriz. *Introduction to Spectroscopy*. Sanat Printers, 3 edition, 2001.

[12] M. Ŝimor, J. RáheÎ, P. Vojtek, et al. Atmospheric-pressure diffuse coplanar surface discharge for surface treatments. *Applied Physics Letters*, 81:2716–2718, 2002. doi:10.1063/1.1513185.

[13] J. F. Kolb, A.-A. H. Mohamed, R. O. Price, et al. Cold atmospheric pressure air plasma jet for medical applications. *Applied Physics Letters*, 92:241501–241503, 2008. doi:10.1063/1.2940325.

[14] R. M. France and R. D. Short. Plasma treatment of polymers: The effects of energy transfer from an argon plasma on the surface chemistry of polystyrene, and polypropylene. a high-energy resolution x-ray photoelectron study. *Langmuir*, 14:4827–4835, 1998. doi:10.1021/la9713053.

[15] C. Canal, R. Molina, E. Bertran, and P. Erra. Study on the influence of scouring on the wettability of keratin fibers before plasma treatment. *Fibers Polymers*, 9:444–449, 2008. doi:10.1007/s12221-008-0071-8.

[16] M. Dhayal, S.-Y. Lee, and S.-U. Park. Application of low-temperature substrate bonding in fabrication of reusable micro-fluidic devices. *Vacuum*, 80:499–506, 2006. doi:10.1016/j.vacuum.2005.06.008.

[17] E. Bormashenko, R. Grynyov, Y. Bormashenko, and E. Drori. Cold radiofrequency plasma treatment modifies wettability and germination speed of plant seeds. *Scientific Reports*, 2:741, 2012. doi:10.1038/srep00741.

[18] N. Balcon, A. Aanesland, and R. Boswell. Plasma sources science and technology. 16:217–225, 2007.

[19] Jaeyoung Park, I. Henins, Hans Herrmann, and Gary Selwyn. Gas breakdown in an atmospheric pressure radio-frequency capacitive plasma source. *Journal of Applied Physics*, 89:15–19, 2001. doi:10.1063/1.1323754.

[20] M. A. Lieberman and A. J. Lichtenberg. *Principles of Plasma Discharges and Materials Processing*. John Wiley & Sons, 1 edition, 2005. doi:10.1002/0471724254.

[21] C. S. Wong and R. Mongkolnavin. Plasma diagnostics techniques. In *Elements of Plasma Technology*, Springer Briefs in Applied Sciences and Technology. Springer, 2016. doi:10.1007/978-981-10-0117-8_3.

[22] A. Falahat, A. Ganjovi, M. Taraz, M. N. R. Ravari, and A. Shahedi. Optical characteristics of a rf dbd plasma jet in various ar/o2 mixtures. *Pramana – Journal of Physics*, 90:27, 2018. doi:10.1007/s12043-018-1520-6.

[23] A. Sarani, A. Nikiforov, and C. Leys. Atmospheric pressure plasma jet in ar and ar/h2o mixtures: optical emission spectroscopy and temperature measurements. *Physics of Plasmas*, 17:063504, 2010. doi:10.1063/1.3439685.

[24] A. Kramida, Y. Ralchenko, J. Reader, and NIST ASD Team. Nist atomic spectra database, 2018. Online: [2019, March 14]. URL: https://physics.nist.gov/asd.

[25] D. P. Subedi, R. B. Tyata, R. Shrestha, and C. S. Wong. An experimental study of atmospheric pressure dielectric barrier discharge (dbd) in argon. In *AIP Conference Proceedings*, volume 1588, page 103, 2014. doi:10.1063/1.4867673.